

General Disclaimer

One or more of the Following Statements may affect this Document

- This document has been reproduced from the best copy furnished by the organizational source. It is being released in the interest of making available as much information as possible.
- This document may contain data, which exceeds the sheet parameters. It was furnished in this condition by the organizational source and is the best copy available.
- This document may contain tone-on-tone or color graphs, charts and/or pictures, which have been reproduced in black and white.
- This document is paginated as submitted by the original source.
- Portions of this document are not fully legible due to the historical nature of some of the material. However, it is the best reproduction available from the original submission.

(NASA-CR-176049) CONTRIBUTIONS TO THE 19TH
INTERNATIONAL COSMIC RAY CONFERENCE
(Washington Univ.) 31 p HC A03/MF A01

CSC1 03B

N85-32044

THRU

N85-32051

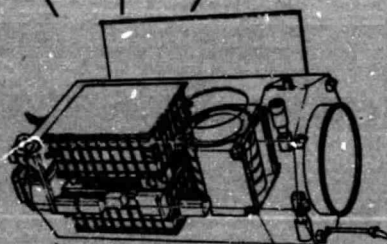
Unclass

G3/88 21851

WASHINGTON
UNIVERSITY
IN ST. LOUIS

STAR 20 AUG 13 1985

HEAO-3
HIGH ENERGY
ASTRONOMY
OBSERVATORY



HEAVY NUCLEI
EXPERIMENT

UNIVERSITY OF MINNESOTA
School of Physics and Astronomy
Minneapolis, Minnesota 55455

CALIFORNIA INSTITUTE OF TECHNOLOGY
Pasadena, California 91125

3
WASHINGTON UNIVERSITY
Dept. of Physics and the
McDonnell Center for the Space Sciences
St. Louis, Missouri 63130

**Contributions to the
19th INTERNATIONAL COSMIC RAY CONFERENCE
La Jolla, California
August 11-23, 1985**

SRL 85 16-22

TABLE OF CONTENTS

- 1) OG 4.1 - 8 Energy Spectra of Elements with $18 \leq Z \leq 28$ Between 10 and 300 GeV/amu
- 2) OG 4.4 - 5 Elemental Abundances of Cosmic Rays with $Z > 33$ as Measured on HEAO-3
- 3) OG 4.4 - 6 Abundances of 'Secondary' Elements among the Ultra Heavy Cosmic Rays - Results from HEAO-3
- 4) OG 4.4 - 7 Lead, Platinum, and other Heavy Elements in the Primary Cosmic Radiation--HEAO-3 Results
- 5) OG 7.1 - 4 Implications of Source Abundances of Ultraheavy Cosmic Rays
- 6) OG 7.2 - 21 Interactions of Heavy Nuclei, Kr, Xe and Ho, in Light Targets
- 7) OG 9.1 - 13 The Response of Ionization Chambers to Relativistic Heavy Nuclei

Papers 1 through 4 are in Volume 2 of the Proceedings; 5 through 7 are in Volume 3.

N85-32045

ENERGY SPECTRA OF ELEMENTS WITH $18 \leq Z \leq 28$
BETWEEN 10 AND 300 GeV/amu

Michael D. Jones^a, J. Klarmann^a, E. C. Stone^b, C. J. Waddington^c, W. R. Binns^a,
T. L. Garrard^b, M. H. Israel^a

^a) Washington University, St. Louis, MO 63130, USA

^b) California Institute of Technology, Pasadena, CA 91125 USA

^c) University of Minnesota, Minneapolis, MN 55455, USA

1. Introduction. The HEAO-3 Heavy Nuclei Experiment (Binns, *et al.*, 1981) is composed of ionization chambers above and below a plastic Cherenkov counter. We have measured the energy dependence of the abundances of elements with atomic number, Z, between 18 and 28 at very high energies where they are rare and thus need the large area \times time of this experiment. We extend the measurements of the Danish-French HEAO-3 experiment (Englemann, *et al.*, 1983) to higher energies, using the relativistic rise of ionization signal as a measure of energy, and determine source abundances for Ar and Ca.

2. Data Analysis. We confine this analysis to events in the $1.1 \text{ m}^2\text{sr}$ in which the cosmic rays penetrate all six ionization chambers, and to the first 314 days of the flight, when all six ionization chambers were functioning properly. These selections give the highest possible ionization resolution. We select only events incident with geomagnetic cutoff greater than 8 GV, so Z is determined by the Cherenkov signal. We further require agreement between the means of the three ionization chamber signals above the Cherenkov and those below, to eliminate most nuclear interactions inside the instrument.

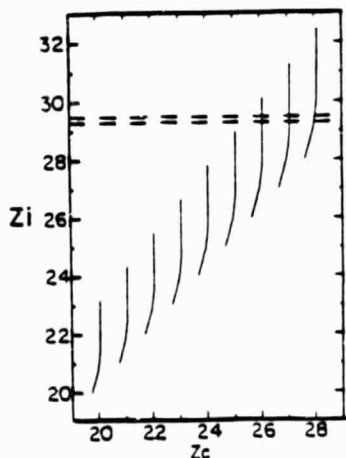


Figure 1

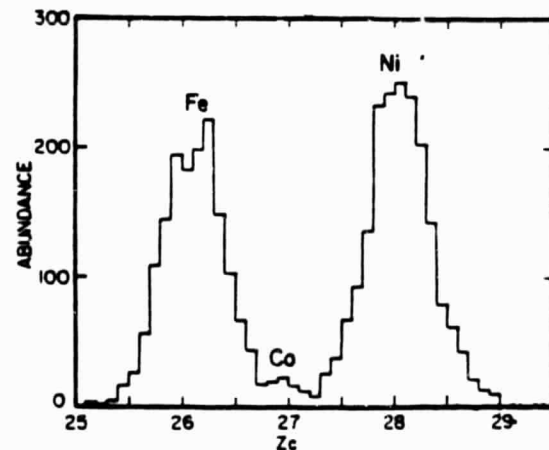


Figure 2

Figure 1 is a schematic plot showing the locus of events for each element, $20 \leq Z \leq 28$. Z_c is the square-root of the Cherenkov signal normalized so $Z_c \approx Z$ at high energy. Z_i is the square-root of the ionization normalized so $Z_i = Z$ at minimum-ionizing. Figure 2 is a histogram of Z_c for events with $29.3 < Z_i < 29.5$, the region between the dashed lines in figure 1. This histogram includes Fe, Co, and Ni at about 130, 34, and 12 GeV/amu respectively. The abundance of each element in each of eighty such histograms is determined by maximum-likelihood fitting.

Corrections to these raw abundances were calculated to account for interactions both in the lid in front of the first ionization chamber and in the Cherenkov counter and other material between the ionization chambers. The latter calculation included only charge changes of one or two charge units, other interactions having been eliminated by the requirement for agreement between upper and lower ionization chambers. The calculation assumed that at all energies the total cross-sections were given by the formula of Westfall *et al.* (1979) and the partial cross-sections for changing by n charge units were the same fraction of the total cross-section for any projectile as was measured by Webber and Brautigam (1982) at 980 MeV/amu for Fe on C. These calculated corrections lowered the raw abundance ratios by typically 10 to 30 percent.

3. Energy Scale. We used Z_i/Z as a measure of energy, and derived an empirical energy calibration by comparing our Fe observations with an Fe energy spectrum derived from a compilation of previously published measurements (Webber, 1982). This Fe spectrum was multiplied by an empirical geomagnetic transmission function which represented the fraction of time when the geomagnetic cutoff permitted Fe of that energy to reach the instrument; the product was the effective Fe spectrum at the instrument, averaged over many orbits. This energy spectrum was then converted to a Z_i/Z spectrum using a trial form of the energy dependence of Z_i/Z . Finally this calculated spectrum was folded with the instrument's ionization resolution, and the resulting Z_i/Z spectrum was compared with the data. The process was iterated, by changing the assumed form of the energy dependence of Z_i/Z , until the calculated and observed spectra of Fe agreed.

The resulting energy dependence is consistent, between about 10 and 100 GeV/amu, with one derived independently for a different detector system by Barthelmy *et al.* (1985, OG 4.1-7). Above about 200 GeV/amu, the shape of our calibration curve depends upon the assumption we made that the Fe energy spectrum falls as a power-law with exponent -2.7 at energies above those where it has been measured.

Abundance ratios derived from data in a particular Z_i/Z histogram were plotted at the mean energy from which those particles came, assuming the Fe energy spectrum and the calibration curve described above. The energy resolution implied by our ionization resolution of 0.40 charge units is comparable to the spacing of the points in figure 3.

4. Results. Figure 3 gives the resulting abundances of several elements relative to Fe as a function of energy. The X symbols are the results of the DF experiment (Englemann, 1983), while the O symbols are the results of this experiment. In every case our results are consistent with those of the DF experiment in the interval where both experiments apply, 10 to 25 GeV/amu. At higher energies our data generally continue the DF trend.

Our data above 10 GeV/amu suggest a Ni/Fe ratio slightly dependent upon energy, with a best fit power law of exponent -0.050 ± 0.016 . If we ignore this slight variation with energy, then the mean value of the Ni/Fe ratio over our data is 0.054 ± 0.001 .

For the secondary ratios, K/Fe, Sc/Fe, Ti/Fe, and V/Fe, our data indicate an extension to about 100 GeV/amu of the same power law dependence as was indicated by the DF data. Figure 4 shows the best fit exponent for each of these ratios combining the DF and our data. The steepening of the slope with decreasing Z is expected as lower Z elements have greater contributions from tertiary nuclei.

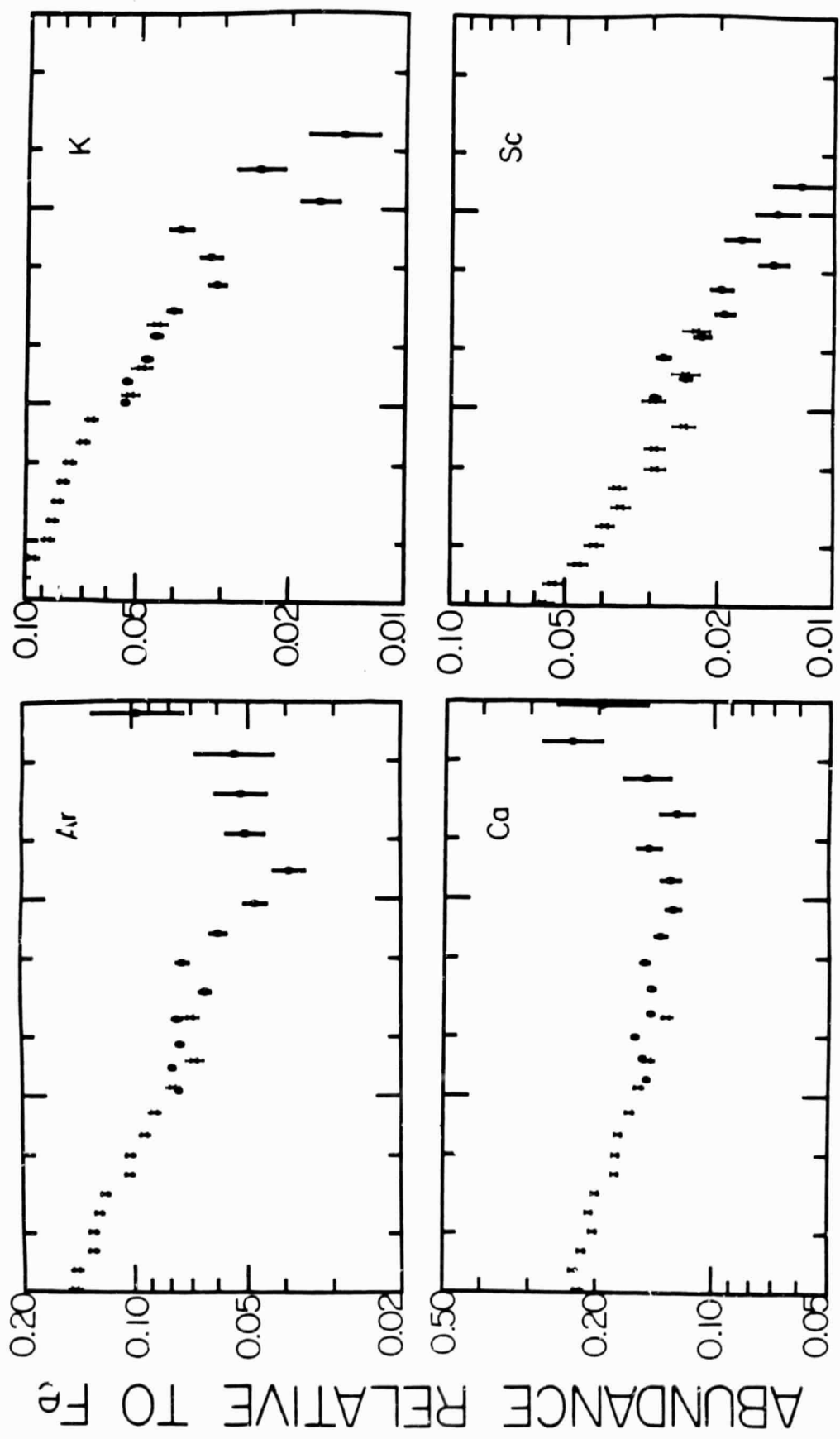
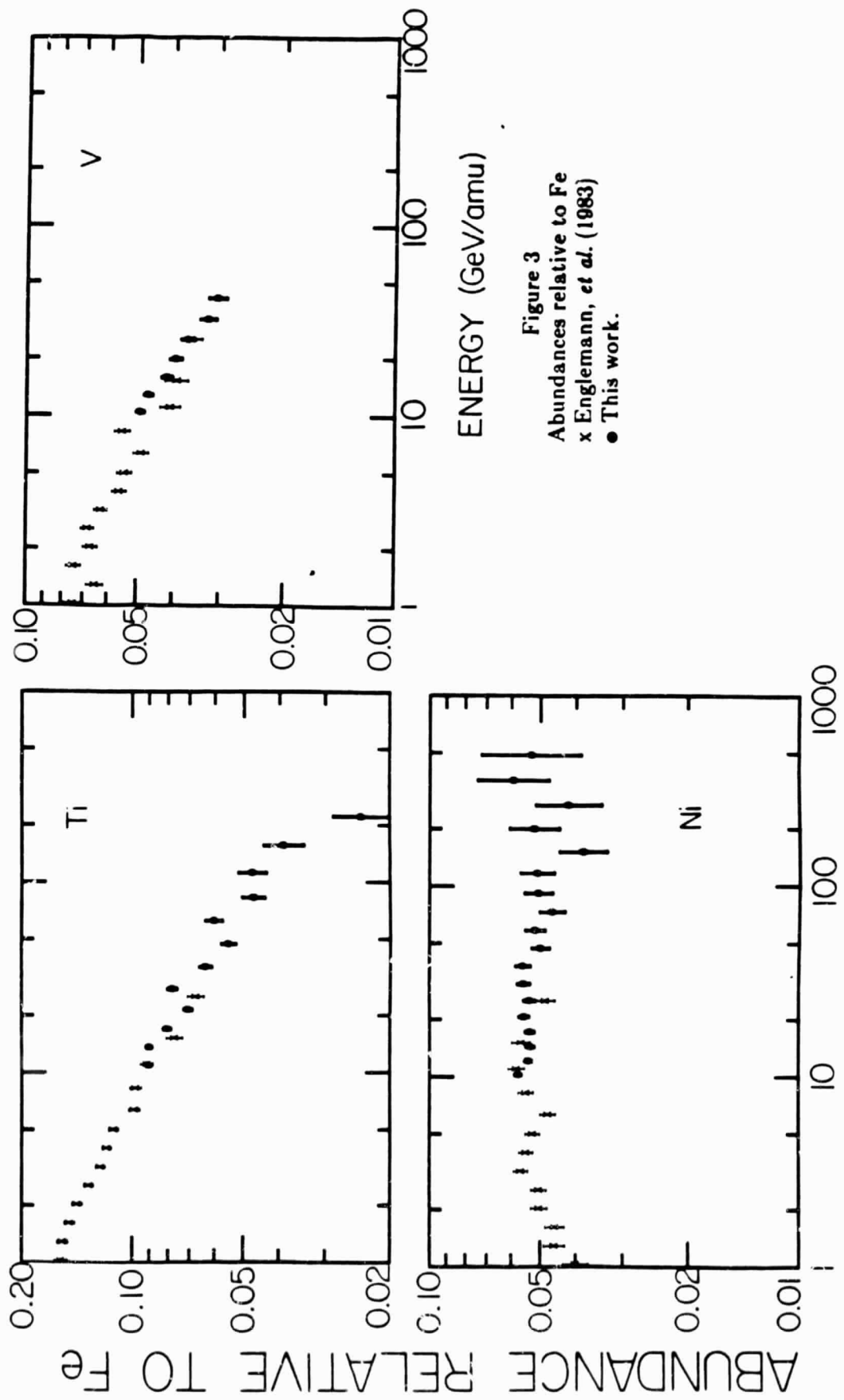


Figure 3
Abundances relative to Fe
 x Englemann, et al. (1983)
 ● This work.



Our data indicate a leveling of the Ca/Fe ratio above the energies of the DF experiment, as would be expected from an energy-independent primary component becoming increasingly significant at higher energies as the secondary component becomes less abundant. We fitted the combination of the DF and our ratios to a function $aE^p + b$. With $p = -0.235 \pm 0.010$, interpolated from figure 4, the result is primary Ca/Fe = 0.094 ± 0.004 . A galactic propagation calculation on the DF data (Lund, 1984) gives a source abundance of Ca/Fe = 0.065 ± 0.019 .

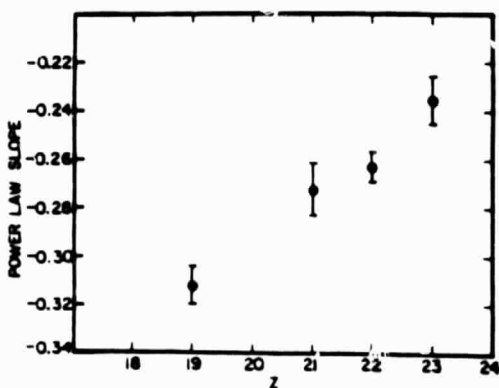


Figure 4
Exponent of power law fit to
abundance of element Z
relative to Fe.

A similar fit to the energy dependence of Ar/Fe, but with $p = -0.33 \pm 0.01$, gives primary Ar/Fe = 0.026 ± 0.003 . Propagation of the DF data (Lund, 1984) gives Ar/Fe = 0.032 ± 0.008 . Source abundances inferred from such galactic propagations on observed abundances 2.5 to 5 times higher must depend critically upon the adopted fragmentation cross-sections, while our extension of observations above 100 GeV/amu permits inference of source abundances without galactic propagation calculations.

5. Acknowledgement. This work was supported in part by NASA grants NAG 8-498, 500, 502, and NGR 05-002-160, 24-005-050, and 26-008-001.

6. References

- Barthelmy, S.D., M.H. Israel, J. Klarmann, 1985, this conference OG4.1-7.
- Binns, W.R., et al., 1981, *Nucl. Instr. Meth.*, 185, 415.
- Englemann, J.J., et al., 1983, *18th ICRC (Bangalore)* 2, 17.
- Lund, N., 1984, *Adv. Space Res.*, 4, (No.2-3), 5.
- Webber, W.R., 1982, *Comp. Origin of Cos. Rays*, ed. M.M.Shapiro, 25.
- Webber, W.R. and D.A. Brautigam, 1982, *Ap. J.*, 260, 894.
- Westfall, G.D., et al., 1979, *Phys. Rev. C*, 19, 1309.

N85-32046**Elemental Abundances of Cosmic Rays with $Z > 33$ as Measured
on HEAO-3**

*B.J. Newport^a, E.C. Stone^a, C.J. Waddington^b, W.R. Binns^c, T.L. Garrard^a,
M.H. Israel^c, and J. Klarmann^c.*

^aCalifornia Institute of Technology, Pasadena, California 91125, USA

^bUniversity of Minnesota, Minneapolis, Minnesota 55455, USA

^cWashington University, St Louis, Missouri 63130, USA

1. Introduction

The Heavy Nuclei Experiment on HEAO-3 (Binns et al., 1981) uses a combination of ion chambers and a Čerenkov counter. During analysis, each particle is assigned two parameters, Z_C and Z_I , proportional to the square roots of the Čerenkov and mean ionization signals respectively. Because the ionization signal is double valued, a unique assignment of particle charge, Z , is not possible in general. Our previous work (Binns et al., 1983, 1985, and Stone et al., 1983) has been limited to particles of either high rigidity or low energy, for which a unique charge assignment was possible, although those subsets contain less than 50% of the total number of particles observed. In this paper we discuss the use of the maximum likelihood technique to determine abundances for the complete data set from ~ 1.5 to ~ 80 GeV/amu.

Figure 1 shows the possible values of Z_C and Z_I for elements near iron, and indicates the substantial overlap between adjacent elements, even before smearing by the resolution function. In Figure 2, the curves of Figure 1 have been transformed using the variable Z_C/Z_I instead of Z_I . This transformation simplifies the following data analysis.

2. Analysis

Particles were selected from the full exposure, 580 days, and were required to have a good Čerenkov signal, at least one good ion chamber and a reliable trajectory. These particles were assigned an initial charge estimate, Z_{est} , and 1/40 of those with $Z_{est} > 19.5$ were saved, together with all the remaining particles with $Z_{est} > 30$. The selected particles were binned in a two dimensional histogram, with one axis being the logarithm of Z_C and the other being Z_C/Z_I . Figure 3 shows a contour plot of the region of this histogram near iron.

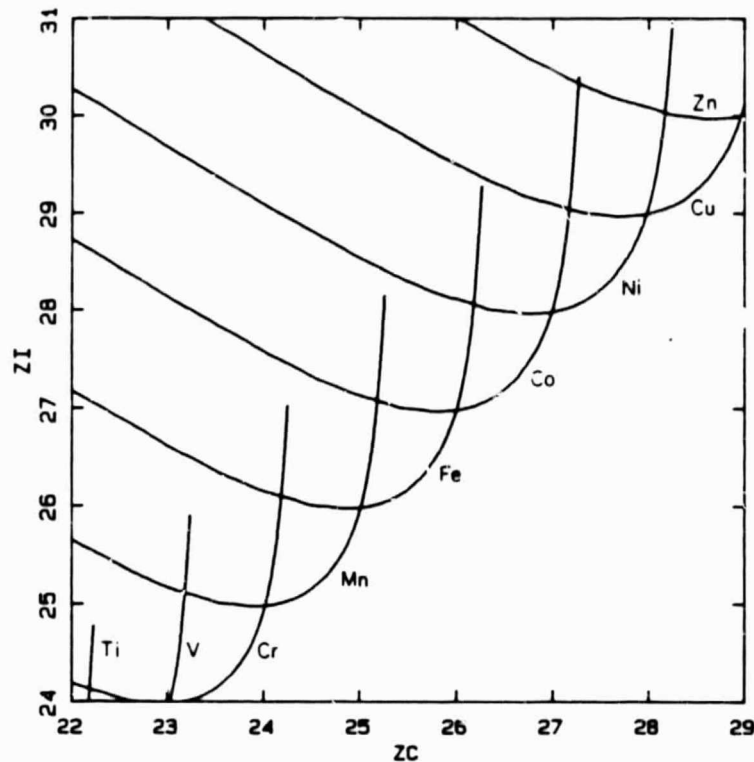


Figure 1. Curves of Z_I versus Z_C for the elements near iron.

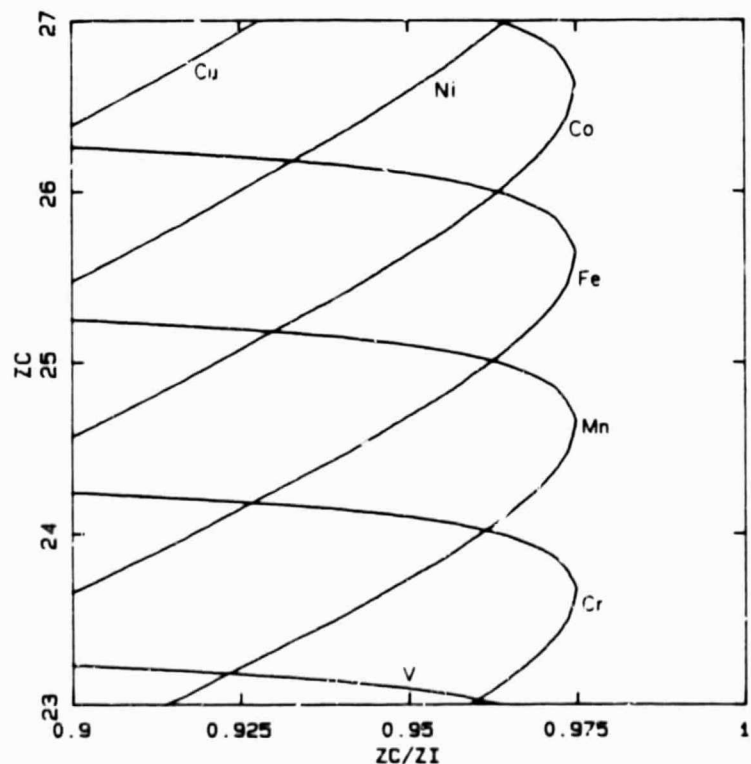


Figure 2. The curves of Figure 1, displayed in $(Z_I/Z_C, Z_C)$ space.

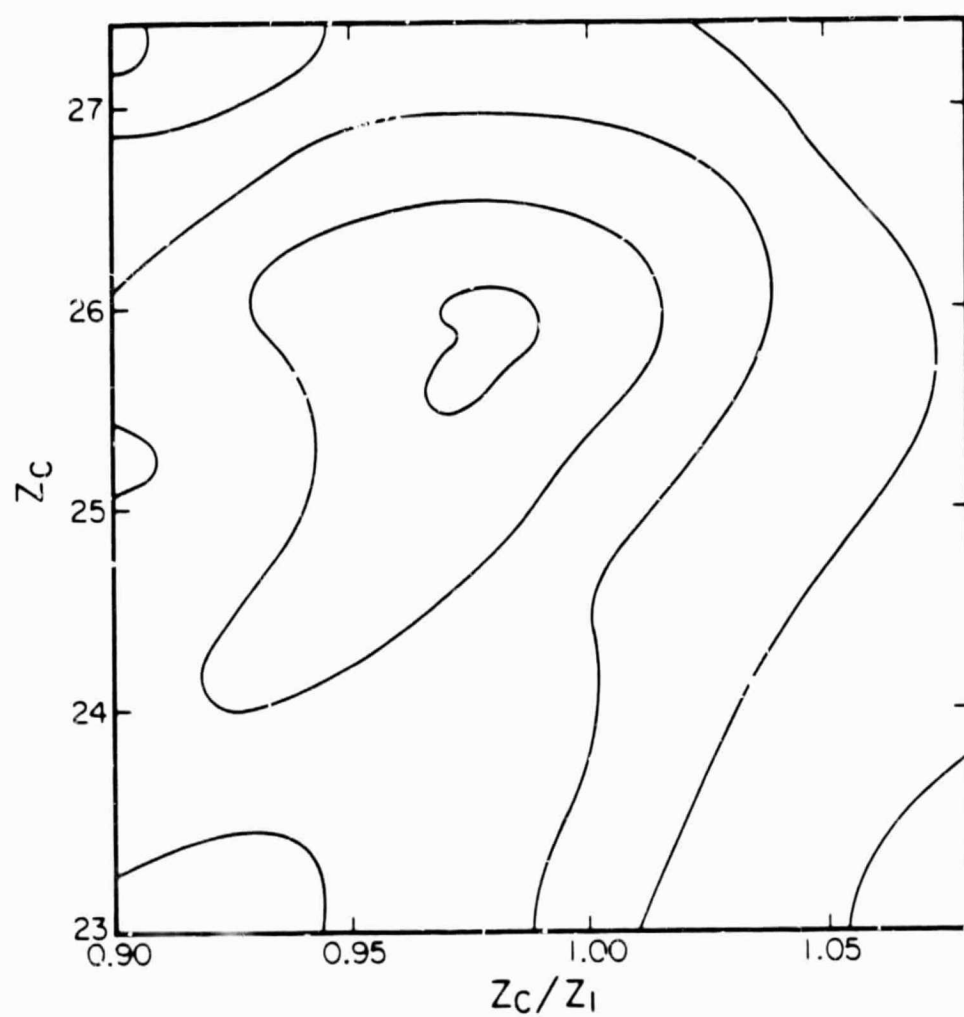


Figure 3. A contour plot of particle density in $(Z_l/Z_C, Z_C)$ space.

We have used the iron distribution as a reference distribution for the other elements, by scaling it according to the following criteria:

- 1) All elements are assumed to have the same energy spectrum, although it is known that the sub-iron secondary elements have steeper spectra (e.g. Jones et al., 1985, OG 4.1-8).
- 2) Energy independent scaling factors have been used.
- 3) The resolution of the instrument is a constant fraction of the signal.
- 4) Non-Z² corrections to the scaling laws for Z_C and Z_C/Z_I have been determined directly from the data.

Those elements contaminating the iron distribution have been approximately removed by scaling the contaminated distribution and subtracting according to an assumed set of abundances. The resulting "clean" iron distribution was smoothed and then scaled to the high Z elements, using cubic interpolation techniques.

The likelihood of a given set of abundances may be calculated using Poisson statistics, and maximized by iterating until all the first derivatives are zero, yielding the best fit. Results from the application of this method will be reported.

3. Acknowledgements

We thank B.W. Gauld for assistance in programming for data analysis. This work was supported in part by NASA grants NAG 8-498, 500, 502 and NGR 05-002-160, 24-005-050, 26-008-001.

4. References

- Binns, W.R., et al., 1981, *Nucl. Inst. Meth.* **185**, 415
Binns, W.R. et al., 1983, *Proc. 18th I.C.R.C. (Bangalore)*, **9**, 106
Binns, W.R., et al., 1985, *Ap. J.* (to be published Oct. 1)
Jones, M.D., et al., 1985, *Proc. 19th I.C.R.C. (San Diego)*, OG 4.4-5
Stone, E.C., et al., 1983, *Proc. 18th I.C.R.C. (Bangalore)*, **9**, 115

N85-32047

**ABUNDANCES OF 'SECONDARY' ELEMENTS AMONG THE
ULTRA HEAVY COSMIC RAYS - RESULTS FROM HEAO-3**

J. Klarmann^a, S. H. Margolis^a, E. C. Stone^b, C. J. Waddington^c,
W. R. Binns^a, T. L. Garrard^b, M. H. Israel^a and M. P. Kertzman^c

^aDepartment of Physics and the McDonnell Center for the Space Sciences,
Washington University, St. Louis MO 63130, USA.

^bGeorge W. Downs Laboratory, California Institute of Technology,
Pasadena CA 91125, USA.

^cSchool of Physics and Astronomy, University of Minnesota,
Minneapolis MN 55455, USA.

1. Introduction. This paper discusses observations of the abundances of elements of charge $62 \leq Z \leq 73$ in the cosmic radiation from the HEAO-3 Heavy Nuclei Experiment (HNE). These elements, having solar, and presumably source, abundances much less than the heavier Pt and Pb groups, are expected to be largely products of spallation. Thus they are indicators of the conditions prevailing during the propagation of cosmic rays. The abundances have changed from those reported previously (Klarmann et al., 1983) due to a different data selection (Binns et al., 1985). This resulted in better charge resolution and in a higher mean energy for the particles. All the particles we have included in this paper were required to have had a cutoff rigidity $R_c > 5$ GV. This allowed the charge determination to be based solely on the Cherenkov measurement. For a description of the detector see Binns et al., (1981).

2. Analysis. The data selection in this paper is identical to that of Waddington et al., (1985, OG4.4-7). We have considered only the following physically significant groups of charges:

Name	Abbreviation	Range	Number observed
Lead and Platinum	PbPt	$74 \leq Z \leq 86$	52
Heavy secondary	HS	$70 \leq Z \leq 73$	10
Light secondary	LS	$62 \leq Z \leq 69$	34

Our discussion will be in terms of the ratios: HS/PbPt and LS/PbPt. In the table, column a) shows the results observed in the detector. The correction factor to outside the detector was derived by propagating eight different plausible theoretical abundances outside the detector through slabs of hydrogen approximating the distribution of aluminum traversed by the particles going into and through the detector. The change of the abundance ratios from outside the detector to inside was nearly independent of the original ratios and is given as a multiplicative correction factor in column b). The abundance outside the detector, column c) is the product of columns a) and b).

Ratio	HEAO Results			Ariel	HEAO/Ariel
	Inside Detector a)	Correction Factor b)	Outside Detector c)	Outside Detector d)	Outside Detector e)
HS/PbPt	0.19 ± 0.07	0.85 ± 0.02	0.16 ± 0.06	0.27 ± 0.07	0.59 ± 0.27
LS/PbPt	0.65 ± 0.14	0.87 ± 0.02	0.57 ± 0.12	0.88 ± 0.15	0.65 ± 0.18

Results from the Ariel-6 UH-nuclei detector which was exposed in a 55° inclination orbit (Fowler et al., 1984) are given in column d), while column e) gives the ratio of our HEAO results to those of Ariel. It is seen that for both ratios our result is about 60%

to 65% that of Ariel's. While these differences are only significant at a level of 1.5 to 2.0 standard deviations, it is unlikely that they are just statistical fluctuations. The data of Ariel extend to significantly lower energy than ours. At lower energies the abundance of secondaries is expected to be greater since both the interaction cross sections and the escape length are larger. We cannot tell yet whether this energy dependence is sufficient to explain the difference.

3. Comparison with Models. The abundance ratios can be compared with predictions of various models. The source abundance used was either the solar system abundances of Anders and Ebihara (1982) (No FIP) or the same adjusted for an exponential dependence (Brewster et al., 1983a) on the first ionization potential (FIP). These were then propagated through the interstellar medium, assuming a leaky-box model, and using the revised code of Brewster et al., (1983a, 1985) with a rigidity dependent escape length (Ormes and Protheroe, 1983) that is 6.21 g/cm of hydrogen at 7 GV. The calculated values are for approximately the same mix of rigidities as the HEAO data. A different model of FIP fractionation (Cook et al., 1979; J. P. Meyer, 1981), in which the cosmic ray source is suppressed by a constant factor relative to solar abundances for elements with ionization potential above 9 eV, yields propagated abundance ratios which in this charge range, are indistinguishable from those of the unfractionated source. Similarly, propagation of an r-process source abundance yielded ratios which in this charge region were close to those from a solar system source. Neither of the last two results is plotted in figure 1.

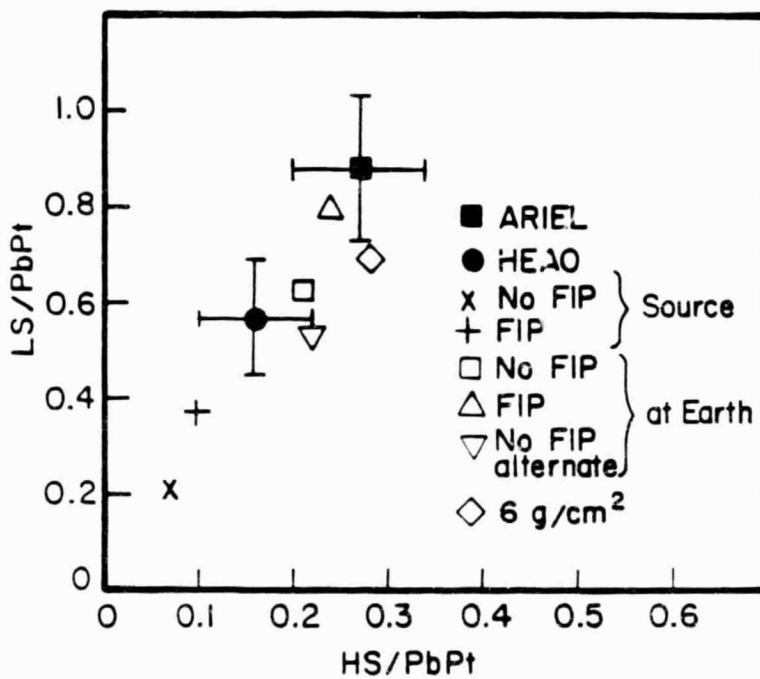


Figure 1: Comparison of the observed and predicted abundance ratios.

In the 'No FIP alternate' propagation an independent code was used (Margolis, 1983) to predict the abundance ratios after propagation through leaky boxes of various escape lengths. The results were then combined using the same rigidity dependent escape length distribution as above to yield the inverted triangle point in figure 1. With this rigidity dependent distribution the mean escape length encountered by the observed particles is $\sim 3\text{g}/\text{cm}^2$. This point, when compared to the other No FIP point, is an

indication of the variation possible in the propagation calculation. The point labeled '6 g/cm²' in figure 1 is the result of the same propagation through a leaky box with a single escape length of 6 g/cm² of hydrogen. The difference between this point and the 'alternate' point shows the dependence of the results on the escape-length distribution. In figure 1 experimental values are solid with error bars.

The dependence of the abundance ratio on propagation can also be demonstrated in a different way. Every point in figures 2 and 3 (Margolis and Blake, 1985) corresponds to the calculated ratio after propagation of a solar system source without FIP through hydrogen with a mean free path distribution rising linearly from zero to the desired 'truncation' then falling exponentially with the given 'escape length' (Margolis, 1983).

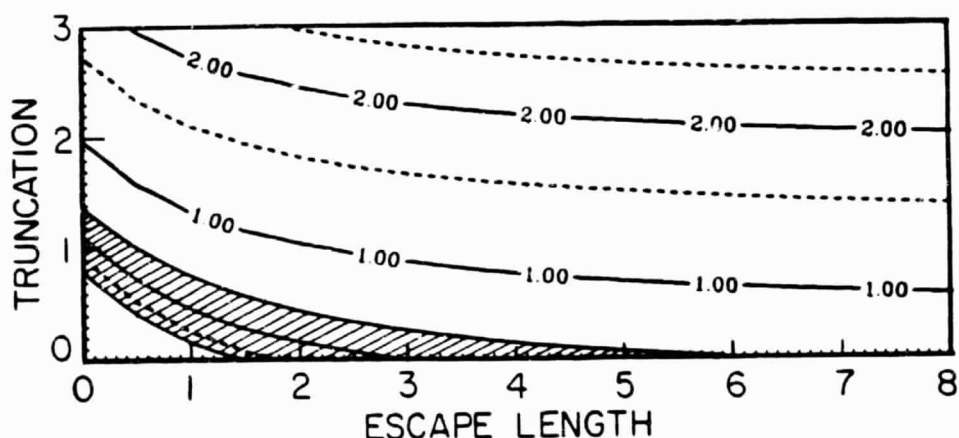


Figure 2: LS/PbPt

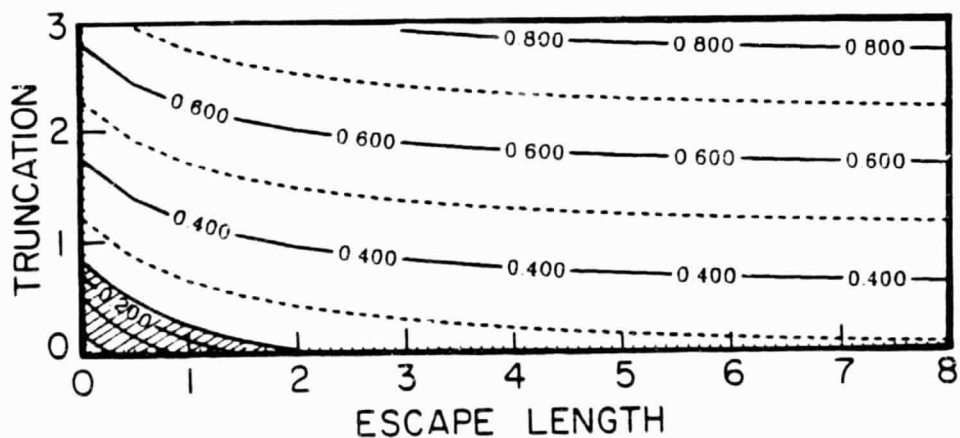


Figure 3: HS/PbPt

In contrast to the data in figure 1, these figures assume that all particles traverse the same path length distribution. Our results are represented by the cross-hatched region yielding possible combinations of escape length and truncation.

As expected the predictions in this charge region are nearly independent of escape-length since the interaction mean free path is so short. However the results do not agree with more than a minute amount of truncation of short path lengths. The fact that at zero truncation an escape length of $\sim 2g/cm^2$ is indicated seems to support the rigidity dependent escape length proposed by Ormes and Protheroe, (1983).

4. Discussion. Our observed values of the secondary ratios are in reasonable agreement with the prediction based on a model without FIP fractionation or with a step function FIP fractionation at the source; however, our observations are in distinct disagreement with the models that include exponential FIP fractionation. This is contrary to the conclusions found at lower charges (Binns et al., 1982, 1983) where observed abundances agreed better with those expected from a solar system source with FIP fractionation than without. Thus other representations of source fractionation may be involved.

Our results do fit the predictions obtained using the standard leaky box model in this energy range. The applicability of this model to lower energies requires further investigation.

5. Acknowledgements: This work was supported in part by NASA grants NAG 8-448, NAG 8-498, 500, 502 and NGR 05-002-160, 24-005-050, 26-008-001.

6. References:

- Anders, E., and Ebihara, M., 1982, *Geochimica et Cosmochimica Acta*, **46**, 2363.
Binns, W. R. et al., 1981, *Nucl. Inst. Meth.*, **185**, 415.
_____, 1982, *Ap.J. (Letters)*, **247**, L115.
_____, 1983, *Ap.J. (Letters)*, **267**, L93.
_____, 1985, *Ap.J.* **297**, in press.
Brewster, N. R., Freier, P.S. and Waddington, C.J., 1983a, *Ap.J.*, **264**, 324
Brewster, et al., 1983b, 18th ICRC, Vol. 9, p. 259.
Brewster, N.R., Freier, P. S. and Waddington, C. J., 1985, *Ap.J.* **294** in press.
Cook, W. R., et al., 1979, 16th ICRC, Vol. 12, p. 265.
Fowler, P. H. et al., 1984, 9th European Cosmic Ray Symposium.
Klarman, J. et al., 1983, 18th ICRC Vol. 9, p.279.
Margolis S. H., 1983, 18th ICRC, Vol. 9, p. 267.
Margolis, S. H. and Blake, J. B., 1985, *Ap. J.* (in press).
Meyer, J. P., 1981, 17th ICRC, Vol. 2, p. 281.
Ormes, J. F., and Protheroe, R. J., 1983, *Ap.J.* **272**, 756.
Silberberg, R., and Tsao, C. H. 1983, *Ap.J. Supp.* **25**, 315 and 335.
Waddington, C. J. et al., 1985, this conference, paper OG 4.4-7.

LEAD, PLATINUM, AND OTHER HEAVY ELEMENTS
IN THE PRIMARY COSMIC RADIATION--HEAO-3 RESULTS

C.J. Waddington,¹ W.R. Binns,² N.R. Brewster,¹ D.J. Fixsen,¹
T.L. Garrard,³ M.H. Israel,² J. Klarmann,² B.J. Newport,³ E.C. Stone³

¹School of Physics and Astronomy, University of Minnesota,
Minneapolis, MN 55455

²Department of Physics and the McDonnell Center for the Space
Sciences, Washington University, St. Louis, MO 63130

³George W. Downs Laboratory, California Institute of Technology,
Pasadena, CA 91125

1. Introduction. This paper reports an observation of the abundances of cosmic-ray lead and platinum-group nuclei using data from the HEAO-3 Heavy Nuclei Experiment (HNE) which consisted of ion chambers mounted on both sides of a plastic Cherenkov counter (Binns et al., 1981). Previously we have reported on a search for actinide nuclei, $Z > 88$ (Binns, et al. 1982a). Further analysis with more stringent selections, inclusion of additional data, and a calibration at the LBL Bevalac, have allowed us to obtain the abundance ratio of lead and the platinum group of elements for particles that had a cutoff rigidity $R_c > 5$ GV.

2. Analysis. We have analyzed 580 days of exposure and considered selected data for those events where the Cherenkov detector and at least two of the ion chambers were triggered. These selection criteria will be described elsewhere, Binns et al. (1985).

Two sets of events satisfying the selections were formed--one for which $Z > 49.5$; the other, a "normalization" set, with 1/400 of all events with $Z > 19.5$, chosen at random.

The events were separated into two groups, 67% with $R_c > 7$ GV and 33% with $5 < R_c < 7$ GV. The charge scale and resolution for each group were determined independently by examining the iron peak in the corresponding normalization set.

In both groups, the nuclear charge of each event was inferred from the Cherenkov signal, assuming that the signal was simply proportional to Z^2 , Garrard et al. (1983).

Fig. 1 shows the observed charge spectrum. This data set demonstrates an odd-even abundance effect for $50 \leq Z \leq 56$ and a sharp falloff in abundances between 56 and 60, similar to that found previously in a data subset having higher charge resolution (Binns et al. 1983). The 322 nuclei with $Z \geq 50$ used in this analysis correspond to $(9.6 \pm 0.5) \times 10^6$ iron nuclei which satisfy the same selection criteria and are observed within

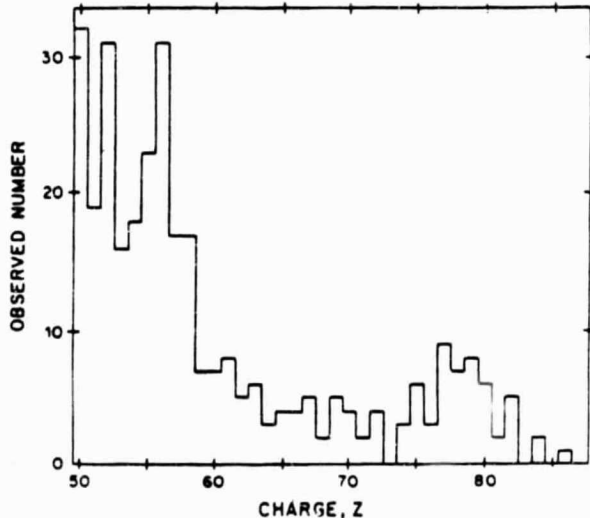


Fig. 1. Observed charge spectrum with charges assigned assuming a Z^2 dependence of the Cherenkov signal.

the instrument, not in free space. The quoted uncertainty is predominately due to the uncertainty in resolving ^{25}Mn from ^{26}Fe .

3. Comparison with Other Data. Results that cover this charge range have been reported from the Ariel-6 UH-nuclei detector which was exposed in a 55° inclination orbit (Fowler et al. 1984), and hence extends to appreciably lower energies than our data. In order to analyze the Ariel data, Fowler et al. had to deconvolve their data using an extrapolation of the resolution function found for Fe and lighter nuclei. We have not attempted a deconvolution of our charge spectrum, since the results of such a process are quite sensitive to the form of the assumed resolution function, particularly when individual element peaks are not apparent in the data. Due to our limited charge resolution we have considered only the following physically significant groups of charges:

Name	Abbreviation	Range	Number observed
"Lead"	Pb	$81 \leq Z \leq 86$	10
"Platinum"	Pt	$74 \leq Z \leq 80$	42

The ratio of the abundance of lead to platinum will be compared with other data and with model predictions. The secondary ratios will be discussed elsewhere, see Klarmann et al. (1985; OG 4.4-6).

The value of 0.24 ± 0.08 for the Pb/Pt ratio derived from our observations differs from that outside the detector because of nuclear interactions during entry and penetration of the detector and the instrumental resolution, which smears the charge distribution. For each of eight plausible models we calculated abundances expected near earth, as described below. Entry into the detector was then simulated by propagation through various slabs of hydrogen approximating the amount of aluminum in the various paths into and through the detector. The resulting element distribution inside the detector was then convolved with the instrument resolution to derive the distribution we would expect to observe. Although the eight models gave very different values for the ratio at the outside of the instrument, the factor by which the ratio changed after propagation into the instrument and convolution with the resolution was nearly the same for all the models. Therefore, we have used a single correction factor of 1.06 ± 0.02 for the ratio.

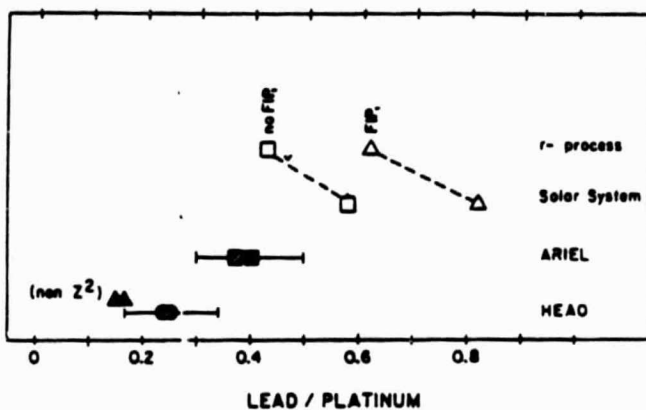
Our resulting ratio of 0.25 ± 0.09 , outside the detector, can be compared with the corresponding result reported by the Ariel experiment of 0.40 ± 0.10 . If this result is combined with those on the secondary ratios, there does seem to be a systematic difference between the two sets of results, although of marginal statistical significance on any individual ratio.

4. Comparison with Models. Our observed charge spectrum, Fig. 1, can be compared with those predicted by various models. A series of predictions were made using the solar system abundances of Anders and Ebihara (1982) and the derived s- and r-process contributions to these abundances. These abundances, taken as calculated, or adjusted for the effects of an exponential dependence on first ionization potential (FIP) fractionation, were used as source abundances. An alternative dependence on FIP, with a step at 9 eV or above, Cook et al. (1979); Meyer (1981), would lead to abundances essentially independent of FIP. These various source abundances were then propagated through the

interstellar medium, assuming a leaky-box model, and using the revised code of Brewster et al. (1983, 1985) with a rigidity dependent escape length (Ormes and Protheroe 1983) that is 6.21 g/cm³ of hydrogen at 7 GV. We have used the cross-sections calculated from the formalism of Silberberg and Tsao (1983). The predictions of this program are in good agreement with the latest predictions obtained by Margolis and Blake (1983), at least for the solar system source abundances.

In Fig. 2, we have shown the calculated values of this ratio for solar system abundances and for r-process abundances; s-process abundances are not given because they show little relation to the observed values with Pb/Pt ratios of ~ 1.0 .

Fig. 2. The "lead to platinum" ratio as observed and predicted. Observed values are shown shaded, while in space values are shown solid and with error bars. The shaded and solid triangles indicate the ratios when a non Z' correction to our charge assignments is included.



Our observed ratio for Pb/Pt (Fig. 2) is distinctly lower than that predicted from solar system source abundances in any of the four models considered. In particular, even considering the models without exponential FIP fractionation, we find an observed ratio that is distinctly lower than that predicted for either a solar-system or an r-process source. This result might suggest that, unlike the cosmic rays with $Z < 60$ (Binns et al. 1982b, 1983), the cosmic rays with Z around 80 come from a source with a distinctly different nucleosynthesis history than do the solar system elements. However, two alternatives to this conclusion must also be considered. First, the Pb abundance in the cosmic ray source may be suppressed by some form of source fractionation which depends upon a different parameter than FIP. Second, it could be that the Pb abundances assumed in our model calculations are not really representative of the solar system or of the r- or s- process contributions to the solar system.

We have noted (Israel et al. 1983) that the cosmic ray abundance of Ge relative to Fe is down by a factor of about two compared to the solar system. Ge, like Pb, is one of the few volatile elements with moderate to low FIP. The factor-of-two underabundance of Ge lends support to the suggestion (Cesarsky and Bibring 1980; Epstein 1980) that it is volatile elements, rather than elements with high FIP, which are underabundant in the cosmic rays. Such a source fractionation dependent on volatility could produce our observed low Pb abundance even with a cosmic ray source whose composition is essentially the same as that of the solar system.

Alternatively, there are reasons for believing that the source abundances of Pb used in our models may not be representative of the solar system values. Our observed Pb/Pt ratio could be consistent with

that expected from a "Pb-poor r-process", either with or without FIP fractionation.

It is possible that the assumed solar system Pb abundance itself is too high. If the Anders and Ebihara Pb abundance were twice that of typical solar system matter, then a solar system source abundance, either with or without FIP fractionation, would agree with our data.

Finally, we note that Ge and Pb, like most elements with higher FIP, have abundances in C2 chondritic meteorites about a factor of two lower than abundances in the C1 chondrites which are the basis for the Anders and Ebihara solar system abundances. If the C2 rather than the C1 chondrites were more nearly representative of the composition of the heavier elements in the solar system, then our low Pb/Pt ratio would again be consistent with a cosmic ray source of composition similar to that of the solar system.

Thus, while our Pb/Pt ratio is distinctly lower than that predicted by any of the standard models for cosmic ray sources, it is possible that the difference is not an indication that the cosmic ray source composition is greatly different from that of the solar system, but rather that there is less Pb in the solar system and in the r-process than is assumed in the standard model.

5. Acknowledgements. The research was supported in part by NASA under grants NAG 8-498, 500, 502, and NGR 05-002-160, 24-005-050, and 26-008-001.

References

- Anders, E., and Ebihara, M. (1982), Geochimica et Cosmochimica Acta, 46, 2363.
Binns, W. R., et al. (1981), Nucl. Inst. Meth., 185, 415.
Binns, W. R., et al. (1982a), Ap.J. (Letters), 261, L117.
_____. (1982b), Ap.J. (Letters), 247, L115.
Binns, W. R., et al. (1983), Ap.J. (Letters), 267, L93.
Binns, W. R., et al. (1984), Adv. Space Res., 4, 25.
Binns, W. R., et al. (1985), to be published in Ap.J., Oct. 1.
Brewster, N. R., Freier, P. S., and Waddington, C. J. (1983), Ap.J., 264, 324.
_____. (1985), to be published in Ap.J., July 1.
Cesarsky, C. J., and Bibring, J. P. (1980), IAU Symposium, 94, 361.
Cook, W. R., et al. (1979), 16th ICRC, Vol. 12, 265.
Epstein, R. I. (1980), MNRAS, 193, 723.
Fowler, P. H., et al. (1984), 9th European Cosmic Ray Symposium.
Garrard, T. L., et al. (1983), 18th ICRC, Vol. 9, 367.
Israel, M. H., et al. (1983), 18th ICRC, Vol. 9, 305.
Klarman, J., et al. (1985), this conf., OG 4.4-6.
Margolis, S. H., and Blake, J. B. (1983), 18th ICRC, Vol 9, 283.
Meyer, J. P. (1981), 17th ICRC, Vol. 2, 281.
Silberberg, R., and Tsao, C. H. (1983), Ap.J. Supp. 25, 315, 335.

IMPLICATIONS OF SOURCE ABUNDANCES OF ULTRAHEAVY COSMIC RAYS

W. R. Binns^a, T. L. Garrard^b, M. H. Israel^a, J. Klarmann^a,
S. H. Margolis^a, E. C. Stone^b, C. J. Waddington^c,

^aWashington University, St. Louis, MO, USA

^bCalifornia Institute of Technology, Pasadena, CA, USA

^cUniversity of Minnesota, Minneapolis, MN, USA

1. Introduction. In this paper we will examine the ratio of cosmic-ray source abundance to solar-system abundance for individual elements. In particular we will look at correlations of these ratios with first-ionization potential (FIP) and also with the expected mass-to-charge ratio (A/Q) of the elements in a million-degree plasma. We have previously examined the FIP correlation and shown that the correlation is affected by the choice of C2 or C1 chondritic meteorites as the solar-system standard for comparison (Binns, *et al.*, 1984). An A/Q correlation was suggested by Eichler and Hainebach (1981), as a consequence of their model of shock acceleration in the hot interstellar medium, and has been examined by Israel (1985). These correlations are presented in the following four figures.

2. Explanation of Figures. Figure 1 plots the ratio of cosmic-ray source to solar-system abundances, normalized to unity for Fe, as a function of the first ionization potential. Error bars indicate the quadratic sum of the error on the solar-system abundance and that on the cosmic-ray source abundance. The element symbols for the various points have been transferred directly below the point.

Cosmic-ray source abundances in all four figures are derived principally from observations on HEAO-3, except for H and He which come from balloon observations (Webber, 1982; Webber and Lezniak, 1974). Two H points are plotted; H(R) uses H abundances at the same rigidity as the other elements; H(E), at the same energy per nucleon. For $6 \leq Z \leq 27$, and for $Z = 29$ and 31 (Cu and Ga), the results are from the Danish-French experiment on HEAO-3 (Lund, 1984). For $Z = 28$ and 30 (Ni and Zn) and for $Z \geq 32$ the results are from the Heavy Nuclei Experiment (Israel, *et al.*, 1983). In each case experimental results were propagated back to the source in a standard leaky-box model.

In figures 1 and 3 the solar system abundances are from Anders and Ebihara (1982). These abundances are mainly from type C1 meteorites; except H, C, N, and O are from photospheric measurements, He is from the solar wind H/He ratio, Ne is from the solar wind Ne/Ar ratio and from astronomical measurements of extra-solar-system nebulae, and Ar, Kr, and Xe are interpolated from nearby elements. In figures 2 and 4 the C1 meteorite abundances are replaced by C2 meteorite abundances (Mason, 1979) in forming the solar-system values.

Figures 3 and 4 have the same ordinates as figures 1 and 2 respectively, but the abscissa is A/Q_{120} , where A is the atomic weight and Q_{120} is the charge state the element would have after removal of all electrons whose ionization potential is less than 120 eV. Thus the abscissa is an estimate of the mass-to-charge ratio which the element would have in a million-degree interstellar gas. (The value 120 eV corresponds to a temperature of 1.4×10^6 K, but the correlation displayed here is insensitive to the precise value of ionization potential selected.)

The implications of these figures will be discussed at the conference.

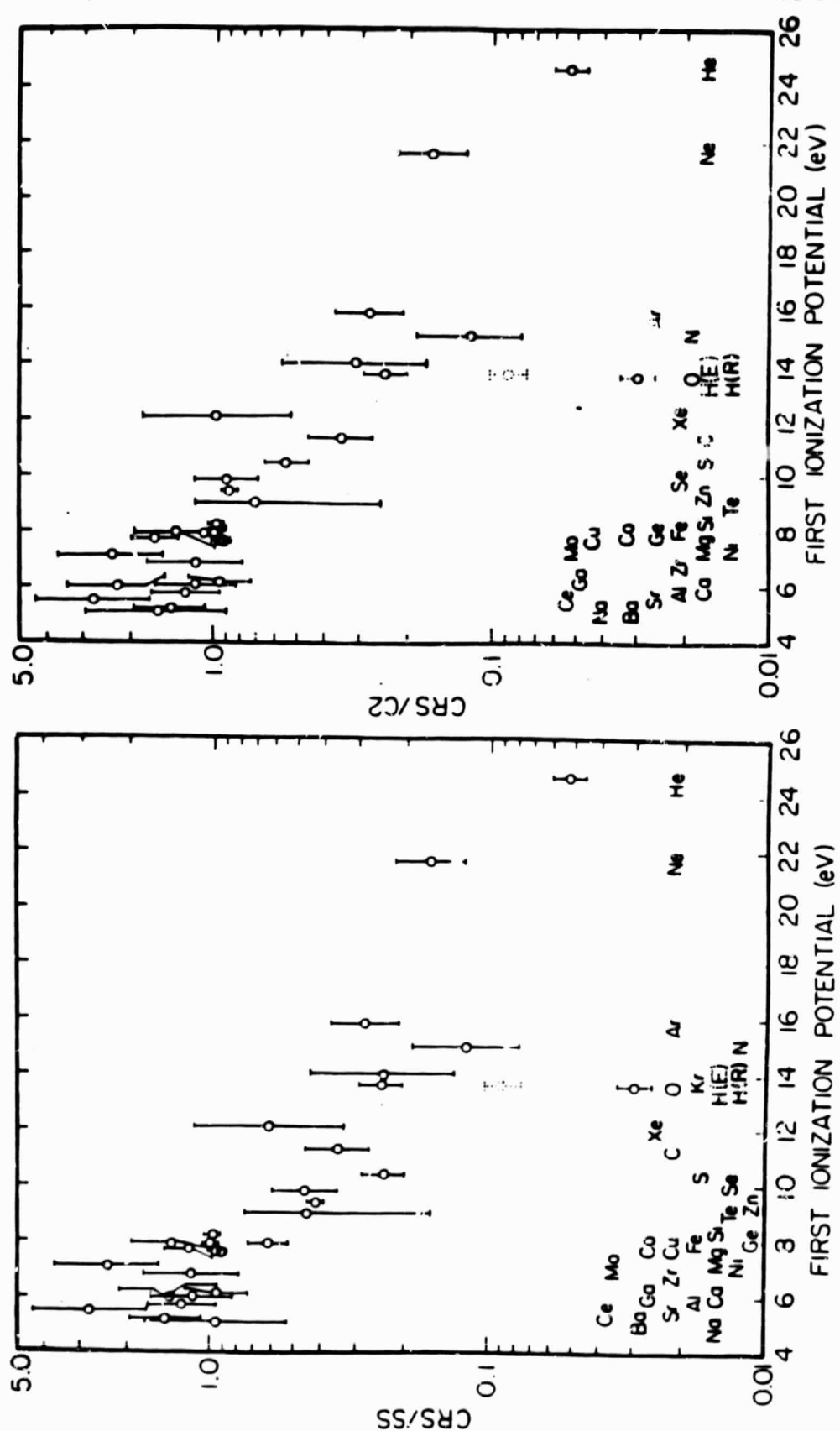


Figure 1

Figure 2

ORIGINAL PAGE IS
OF POOR QUALITY

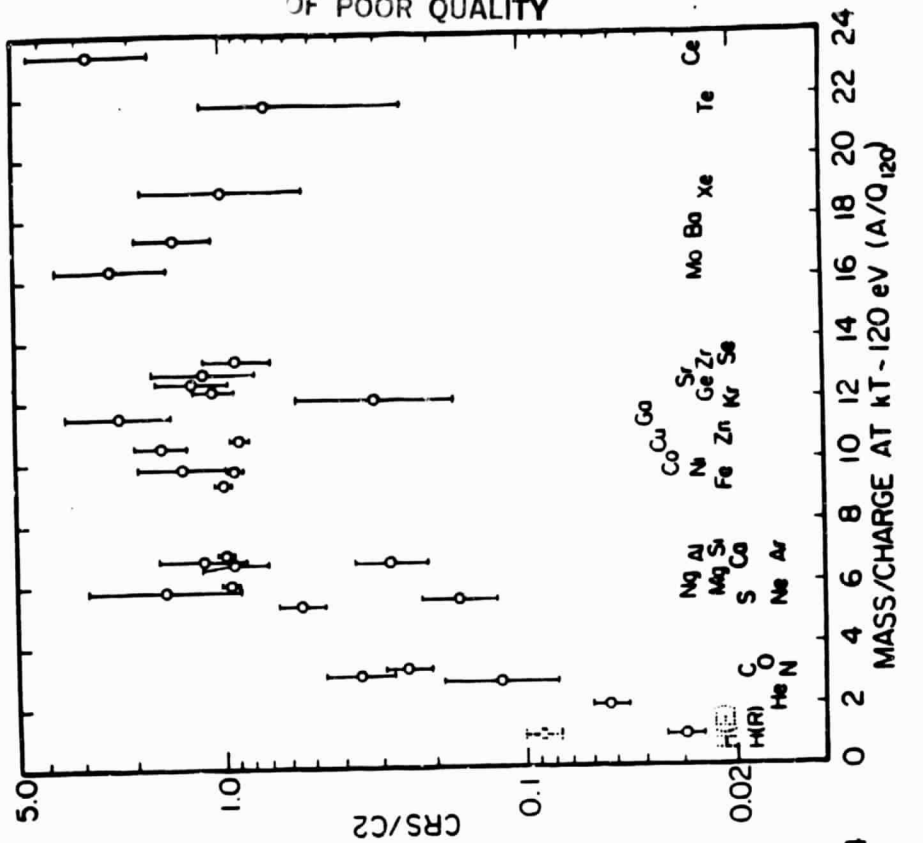


Figure 4

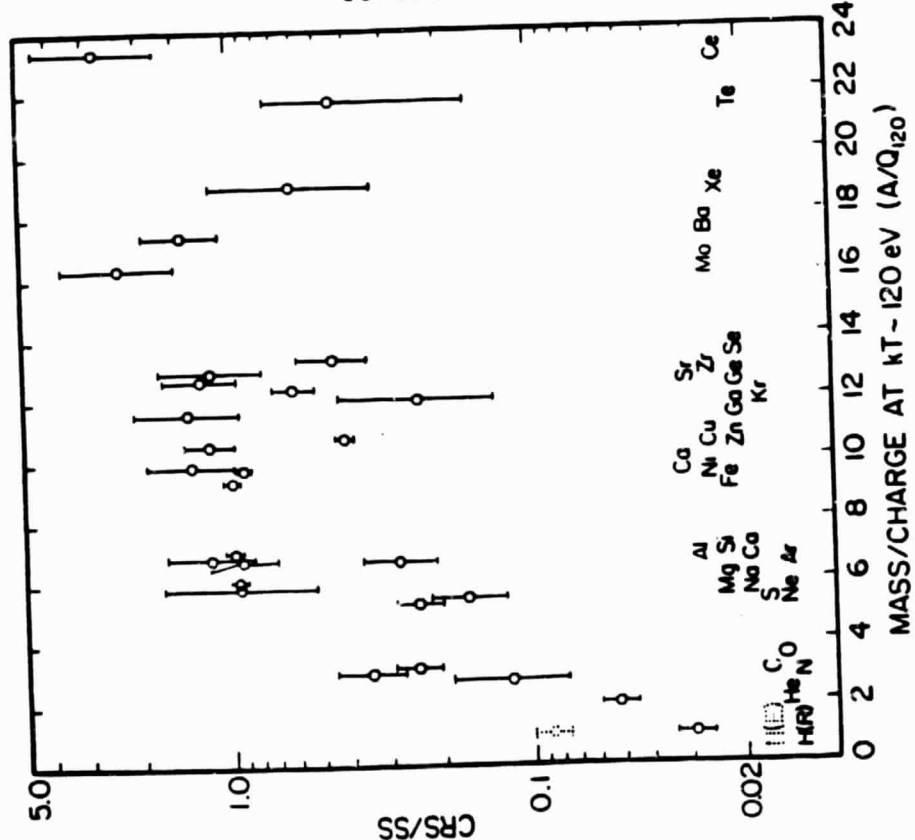


Figure 3

3. References.

- Anders, E. and M. Ebihara, 1982, *Geochim. Cosmochim. Acta*, **46**, 2383.
Binns, et al., 1984, *Adv. Space Res.* **4**, (no. 2-3), 225.
Eichler, D. and K. Hainebach, 1981, *Phys. Rev. Lett.* **47**, 1560.
Israel, M.H., 1985, *12th Texas Symp. Relativistic Astrophys.*, in press.
Israel, et al., 1983, *18th ICRC*, **9**, 305.
Lund, N., 1984, *Adv. Space Res.* **4**, (no. 2-3), 5.
Mason, B., 1979, Geol. Survey Prof. Paper 440-B-1.
Webber, W.R., 1982, *Ap. J.*, **255**, 329.
Webber, W.R. and J.A. Lezniak, 1974, *Ap. Space Sci.*, **30**, 361.

INTERACTIONS OF HEAVY NUCLEI, Kr, Xe AND Ho, IN LIGHT TARGETS

M.P. Kertzman,¹ J. Klarmann,² B.J. Newport,³ E.C. Stone,³
 C.J. Waddington,¹ W.R. Binns,² T.L. Garrard,³ M.H. Israel²

¹School of Physics and Astronomy, University of Minnesota,
 Minneapolis, MN 55455

²Department of Physics and the McDonnell Center for the Space
 Sciences, Washington University, St. Louis, MO 63130

³George W. Downs Laboratory, California Institute of Technology,
 Pasadena, CA 91125

1. Introduction. Over the past few years, we have been analyzing the HEAO-3 measurements of the abundances of ultra-heavy cosmic ray nuclei ($Z > 26$) at earth.¹ In order to interpret these abundances in terms of a source composition, allowance must be made for the propagation of the nuclei in the interstellar medium. Vital to any calculation of the propagation is a knowledge of the total and partial interaction cross sections for these heavy nuclei on hydrogen. Until recently, data on such reactions have been scarce, and we have relied on the semi-empirical formalism of Silberberg and Tsao² to predict the partial cross sections. However, now that relativistic heavy ion beams are available at the LBL Bevalac, some of the cross sections of interest can be measured at energies close to those of the cosmic ray nuclei being observed.

During a recent calibration at the Bevalac of an array similar to the HEAO-C3 UH-nuclei detector, we exposed targets of graphite (C), polyethylene (CH_2), and aluminum to five heavy ion beams ranging in charge (Z) from² 36 to 92. Total and partial charge changing cross sections for the various beam nuclei on hydrogen can be determined from the measured cross sections on C and CH_2 , and will be applied to the propagation problem. The cross sections on Al can be used to correct

Table 1. Number of Events ($\times 10^3$)

Energy (GeV/n):	Kr	Xe	Ho	Au	U
1.5	1.2	1.1	1.0	0.9	

Target:

C	--	210	130	260	60
CH_2	--	330	200	400	90
Al	90	160	190	200	--
"Blank"	35	110	120	260	40

the abundances of UH cosmic rays observed in the HEAO C-3 detector for interactions in the detector itself. Table 1 shows the combinations of beams and targets, as well as the number of events incident on the target for each run. The energies of each beam are also shown. Our preliminary results show that we achieved a charge resolution on the fragments that ranged from 0.21 charge units for Kr on Al to 0.28 c.u. for Au on C, permitting unambiguous resolution of individual fragments. In this paper we report on the total cross sections for Kr on Al, and total and partial cross sections for Xe and Ho on C, CH_2 and H.

2. Experimental Setup. The detector consisted of an array of two front ion chambers, a target space, two rear ion chambers, followed by a Pilot 425 Cherenkov counter. From signals in the front ion chambers, we find

that approximately 10% of the nuclei incident on the detector do not have the nominal charge of the beam, and we eliminate these events from further analysis. Fragments produced in the target as well as beam nuclei surviving through the target are measured in the rear ion chambers and the Cherenkov counter. Scatter plots of the signals in these detectors show well resolved peaks for individual fragments.

3. Total Cross Sections. The interaction mean free path can be found by counting the number of beam nuclei which survive through the target and our detector, and correcting for interactions in the detector itself. This correction is found from a "blank" or no target run. The total interaction cross section per nucleus is related to the mean free path by the following expression:

$$\sigma (\text{mb}) = \bar{A}_T / (6.02 \times 10^{-4}) \lambda (\text{g/cm}^2)$$

where \bar{A}_T is the mean mass number of the target. Our results for the total cross sections are given in Table 2, along with values calculated using the formula from Westfall et al.³ for charge changing cross sections, σ_W . Although this formula was derived from data for nuclei

with $Z \leq 26$, it gives values which only slowly deviate from those measured as Z increases, with $\sigma/\sigma_W = 0.85$ for Ho on H.

Table 2. Total Cross-Sections

Beam	Target	$\lambda(\text{g/cm}^2)$	$\sigma(\text{mb})$	σ_W	σ/σ_W
Kr	Al	19.3	2300 ± 100	2460	.95
Xe	C	8.9	2240 ± 80	2460	.91
Xe	CH_2	5.1	1510 ± 50	1670	.91
Xe	H	1.4	1150 ± 90	1270	.90
Ho	C	7.8	2560 ± 70	2760	.93
Ho	CH_2	4.6	1690 ± 40	1910	.89
Ho	H	1.3	1260 ± 75	1490	.85

4. Partial Cross Sections. The numbers of fragments produced in the target are measured in the rear ion chambers and the Cherenkov counter. A histogram of the

Cherenkov signal for events consistent with their being fragments is shown in Fig. 1. The charge resolution for this particular run is 0.23 charge units.

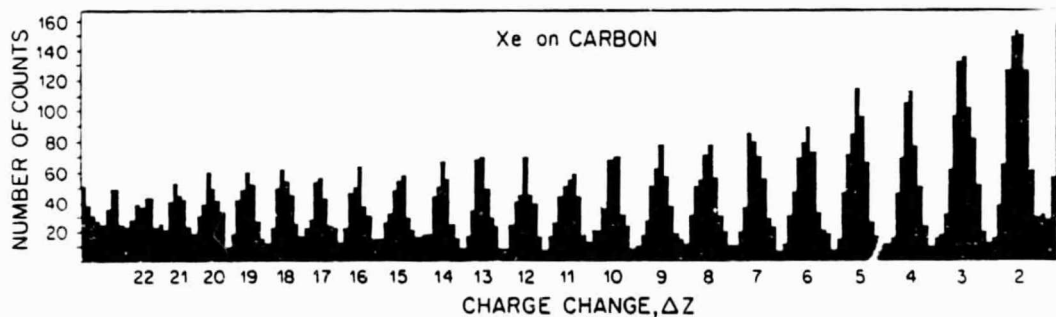


Fig. 1. Cherenkov histogram for Xe nuclei on Carbon.

Several corrections must be applied to the yields obtained from these histograms. First, there is a correction for events observed in the blank run which are also consistent with their being fragments.

These events are due to interactions of the beam in the matter between the Cherenkov counter and the ion chambers. Also, for a given Z, there is a background due to the fragments of charge Z + 1 making a $\Delta Z = 1$ interaction in the Cherenkov counter. Both of these corrections are small, being less than 2%. In addition, there must be a correction for absorption in the detector. We have done this by applying an exponential absorption law, using the Westfall et al.³ charge changing cross section, scaled to our measurements, to calculate the necessary mean free paths. The numbers resulting from this correction are the numbers of each fragment exiting the target. To obtain the partial cross sections from these numbers we need to correct for multiple interactions in the target. The targets used were approximately 0.25 of a mean free path, and were chosen as a compromise between being thick enough to produce a reasonable number of interactions, yet thin enough so as not to degrade the charge resolution of the Cherenkov due to the energy spread of the fragments. We have used a slab propagation program to do this thick target correction.

Table 3 lists the partial cross sections of Xenon and Holmium on C, CH₂, and H. The hydrogen cross sections are derived from the C and CH₂ cross sections per nucleus by a subtraction procedure:

$$\sigma_H = 1/2 (3 \sigma_{CH_2} - \sigma_C)$$

Also given in Table 3 are the values predicted⁴ for Xe and Ho on H. Fig. 2 shows the ratios of our values and those predicted, as a function of ΔZ for Xe and Ho. The errors shown are the statistical errors on the target and blank runs, combined with the errors due to the top of detector correction. Also shown is a fit to previously measured ratios reported for Au nuclei,⁵ showing distinctively different behavior.

Table 3

ΔZ	Xe on C	Xe on CH ₂	Xe on H	S & T	Ho on C	Ho on CH ₂	Ho on H	S & T
1	249±21	230±9	220±17	257	343±35	270±26	234±42	267
2	128±5	137±4	141±6	169	138±5	133±4	131±6	257
3	105±4	104±3	104±5	106	103±4	117±3	124±5	166
4	72±4	94±3	105±5	106	81±4	97±3	105±5	114
5	73±4	79±3	82±5	61	73±3	89±3	97±4	95
6	63±3	73±2	77±4	64	67±3	78±2	84±4	81
7	53±3	65±2	71±4	50	60±3	67±2	71±4	66
8	53±3	53±2	53±1	47	53±3	57±2	59±3	71
9	45±3	47±2	48±3	33	45±3	51±2	54±3	53
10	43±3	43±2	43±3	31	46±3	49±2	51±3	51
11	40±2	37±2	35±3	21	43±3	40±2	38±3	34
12	35±2	33±2	32±3	18	34±2	32±2	31±3	32
13	37±2	31±2	28±3	14	38±2	29±2	24±2	18
14	37±2	27±2	23±3	14	33±2	25±1	20±2	14
15	33±2	20±1	14±2	9	33±2	22±1	17±2	12
16	33±2	19±1	12±2	8	32±2	19±1	13±2	8
17	30±2	17±1	10±2	6	34±2	18±1	10±2	7
18	32±2	16±1	7±2	6	32±2	15±1	7±2	5
19	31±2	15±1	6±2	5	27±2	13±1	6±2	5
20	30±2	13±1	5±2	6	25±2	15±1	10±2	5
21	27±2	13±1	6±2	5	--	--	--	--

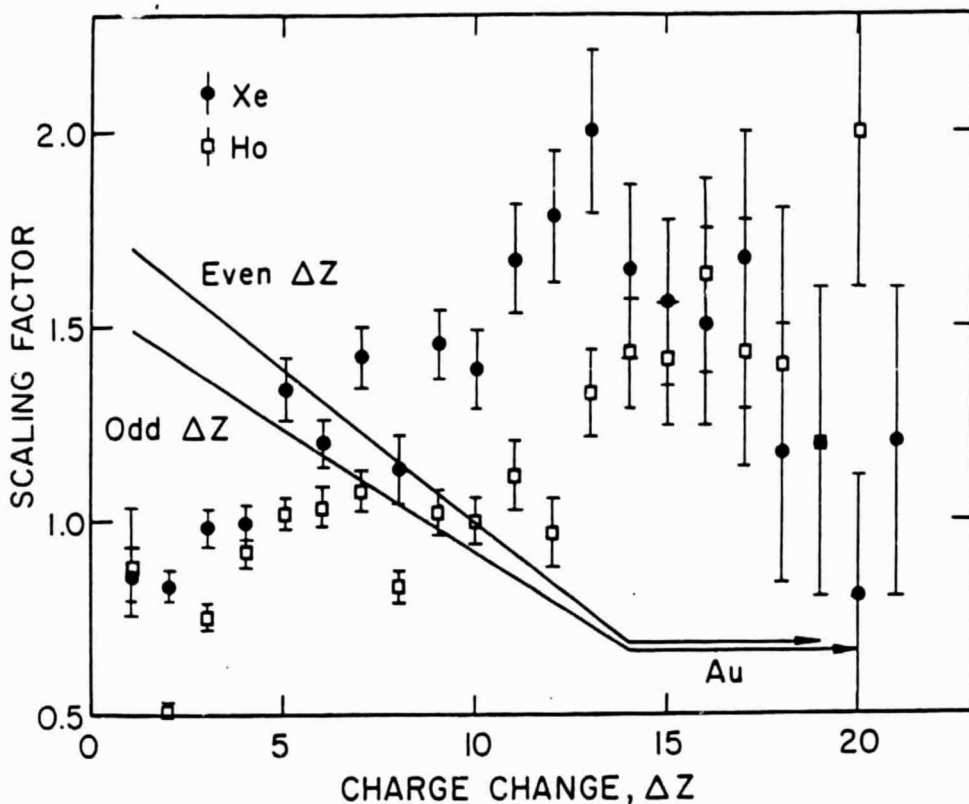


Fig. 2. Ratio of observed to predicted cross-sections as a function of ΔZ .

Examination of these data and of the earlier Au-data from Brewster et al. (1983) shows that they can be well represented by universal curves if expressed as $d\sigma/\sigma_T$ versus ΔZ . We find that for heavy targets, carbon and aluminum, $d\sigma/\sigma_T = a (\Delta Z)^m$ where a and m are closely similar constants for all non-hydrogenous targets and projectiles. Similarly for a hydrogen target, $d\sigma/\sigma_T = b \exp(-n\Delta Z)$, where b and n are closely similar constants for all studied projectiles. The polyethylene targets also show a similar exponential dependence.

4. Acknowledgements. We are grateful to the staff of the LBL Bevalac. This work was supported in part by NASA under grants NAG 8-498, 500, 502, and NGR 05-002-160, 24-005-050, and 26-008-001.

References

- ¹Binns, W. R. et al. (1984), Ap. J. 247, L115; (1983) Ap. J. 267, L93.
- ²Silberberg, R. and Tsao, C. H. (1973), Ap. J. Suppl. 25, 335.
- ³Westfall, G. D. et al. (1979), Phys. Rev. C 19, 1309.
- ⁴Tsao, C. H. and Silberberg, R., (1979), Proc. 16th ICRC (Kyoto), 2, 202.
- ⁵Brewster, N. R. et al. (1983), Proc. 18th ICRC, 9, 259; (1984) Ph.D. Thesis, Univ. of Minn.

N85-32051

The Response of Ionization Chambers to Relativistic Heavy Nuclei

B.J. Newport^a, E.C. Stone^a, C.J. Waddington^b, W.R. Binns^c, D.J. Fixsen^b,
T.L. Garrard^a, G. Grimm^c, M.H. Israel^c, and J. Klarmann^c.

^aCalifornia Institute of Technology, Pasadena, California 91125, USA

^bUniversity of Minnesota, Minneapolis, Minnesota 55455, USA

^cWashington University, St Louis, Missouri 63130, USA

ABSTRACT

As part of a recent calibration at the LBL Bevalac for the Heavy Nuclei Experiment on HEAO-3, we have compared the response of a set of laboratory ionization chambers to beams of ^{26}Fe , ^{36}Kr , ^{54}Xe , ^{67}Ho , and ^{79}Au nuclei at maximum energies ranging from 1666 MeV/amu for Fe to 1049 MeV/amu for Au. The response of these chambers shows a significant deviation from the expected energy dependence, but only a slight deviation from Z^2 scaling.

1. Introduction

Gas filled ionization chambers were used on the Heavy Nuclei Experiment (HNE) on HEAO-3 (Binns et al., 1981). The response of such chambers is expected to be proportional to the energy deposited by the particle traversing them. At low energies this energy deposit is simply the ionization energy loss, while at high energies energetic knockon electrons are able to escape from the chamber, reducing the energy deposit.

To first order the ionization energy loss scales as the square of the particle charge Z , however at high Z this assumption breaks down. A more complete expression is given by Ahlen (1980, 1982), and predicts an energy loss rising slightly faster than Z^2 . Such effects are important when identifying ultraheavy elements.

We have performed two calibrations of ion chambers at the LBL Bevalac using beams ranging from ^{25}Mn to ^{79}Au . The first, in 1982, was done with a prototype of the HNE ion chamber module which was essentially identical to that used in flight. Thus those data, reported in Garrard et al., 1983, are directly applicable to our flight experience at the energies calibrated. The second calibration, in 1984, used lab chambers which were made of thinner and more uniform materials, permitting better resolution and better knowledge of the beam energy in each ion chamber, at the cost of less direct relevance to the flight data. Figure 1 is a schematic drawing of the 1984 detector.

Particles entering the 1984 detector traversed $\sim 0.1 \text{ g cm}^{-2}$ of mylar in the upstream window, rather than the $\sim 1 \text{ g cm}^{-2}$ of aluminum honeycomb in the flight prototype; thus the energy loss in the window is much smaller and more uniform. Also, in the 1984 calibration the beam energy was measured with a magnetic spectrometer after being degraded to the calibration energy, rather than being calculated from an energy loss model.

The lab ion chambers had aluminized mylar electrodes (0.8 mg cm^{-2}) rather than aluminum screenwire (10 mil diameter, 62.5 mil spacing); thus the production and absorption of knockons is much more uniform. A Monte Carlo model of knockon

production correctly predicts the degradation in resolution caused by non-uniform production of knockons in the screen wire electrodes. This resolution degradation in the flight chambers tends to mask the relatively subtle deviations from Z^2 scaling.

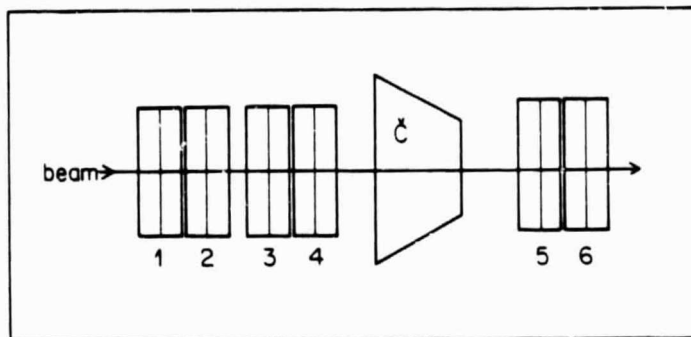


Figure 1. Schematic drawing of the 1984 detector, showing the six ion chambers.

In 1982 the ultraheavy capabilities of the Bevalac were new and we calibrated only on beams of ~ 1700 MeV/amu ^{25}Mn and ~ 1000 MeV/amu ^{79}Au . The 1984 calibration used beams of ^{26}Fe , ^{36}Kr , ^{54}Xe , ^{65}Ho , and ^{79}Au at maximum energies ranging from 1666 MeV/amu for Fe to 1049 MeV/amu for Au.

2. Results of the 1984 Calibration

Figure 2 shows the response of chambers 1, 5, and 6 to ^{26}Fe nuclei as a function of the energy at the midplane of the appropriate chamber, and compares their signals to the calculated dE/dx , arbitrarily normalized at 500 MeV/amu (requiring 27.9 eV per ion pair in the P-10 gas used (90% argon, 10% methane)). It is apparent that the signals fall below that predicted by dE/dx at energies above 700 MeV/amu. This loss of signal is somewhat surprising since at these energies we would expect knockons escaping from the exit window to be in equilibrium with those arriving from above, particularly for chambers 5 and 6 which have $\sim 2 \text{ g cm}^{-2}$ of upstream material. However, some of the decrease in observed signal may be due to knockons escaping from the sides of the chambers.

By interpolating to a particular energy we can construct a plot of signal versus Z at that energy. At low energies, the heaviest nuclei have an effective charge, $Z_{\text{eff}} = Z[1 - \exp(-130\beta Z^{-2/3})]$, due to electron capture (Pierce and Blann, 1968). Figure 3 shows the pulse heights, scaled down by Z_{eff}^2 , at four energies for $Z = 26-79$, using ion chambers 1, 5, and 6. The uranium data have not been included because the charge state in the magnetic spectrometer was uncertain for those beams whose energy had been degraded significantly. The straight lines represent a linear fit to the data, and it is apparent that there is a small negative non- Z^2 effect. The charge of an ^{82}Pb nucleus would be underestimated by about 0.5 charge units at these energies, in contrast with the charge overestimate of +3 charge units observed in the calibration of the flight chambers.

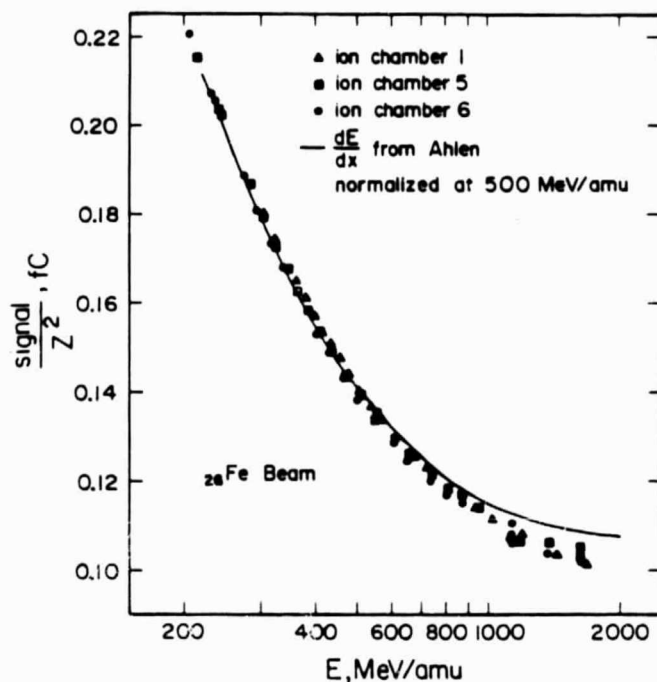


Figure 2. The response of chambers 1, 5, and 6 to ^{26}Fe nuclei as a function of energy.

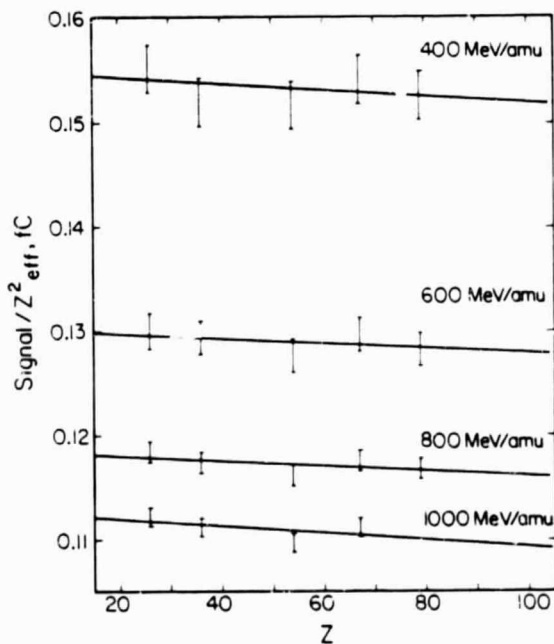


Figure 3. Response of chambers 1, 5, and 6 at four energies, scaled by Z_{eff}^2 .

3. Conclusions

Although the non-Z² effects in these chambers differ from those observed in the prototype flight chambers, the assumption of Z² scaling is still not seriously in error. We also note that our published abundances above charge 50 have used primarily the Čerenkov detector to assign charges, and are unaffected by small non-Z² effects in the ion chambers.

Since the two calibrations differ, the ionization response to energy loss must be sensitive to details of the mass distribution above, below, and within the chambers. As a result we have used the flight data to directly determine both the energy dependence and effective non-Z² correction (Jones et al., (1985, OG 4.1-8) and Newport et al., (1985, OG 4.4-5)).

4. Acknowledgements

The success of this calibration was largely due to the efforts of the staff at LBL, especially Hank Crawford, Mel Flores, Peter Lindstrom, and Fred Lothrop. John Epstein provided invaluable assistance in constructing and aligning the instrument. This work was supported in part by NASA contracts NAS 8-27976, 77, 78, and grants NAG 8-498, 500, 502 and NGR 05-002-160, 24-005-050, 26-008-001.

5. References

- Ahlen, S.P. 1950, *Rev. Mod. Phys.* **52**, 121
- Ahlen, S.P. 1982, *Phys. Rev. A* **25**, 1856
- Binns, W.R., et al., 1981, *Nucl. Inst. Meth.* **185**, 415
- Garrard, T.L. et al., 1983, *Proc. 18th I.C.R.C. (Bangalore)*, **9**, 367
- Jones, M.D. et al., 1985, *Proc. 19th I.C.R.C. (San Diego)*, OG 4.1-8
- Newport, B.J. et al., 1985, *Proc. 19th I.C.R.C. (San Diego)*, OG 4.4-5
- Pierce, T.E. and Blann, M. 1968, *Phys. Rev.* **173**, 390